Available online at www.sciencedirect.com
ScienceDirect
Trans. Nonferrous Met. Soc. China 24(2014) 2536−2543
Transactions of Nonferrous Metals Society of China
www.tnmsc.cn

Creep properties and microstructure evolution of nickel-based single crystal superalloy at different conditions

Zhen-xue SHI, Jia-rong LI, Shi-zhong LIU, Xiao-guang WANG

Science and Technology on Advanced High Temperature Structural Materials Laboratory, Beijing Institute of Aeronautical Materials, Beijing 100095, China

Received 29 July 2013; accepted 17 December 2013

Abstract: The creep properties of nickel-based single crystal superalloy with [001] orientation was investigated at different test conditions. The microstructure evolution of γ' phase, TCP phase and dislocation characteristic after creep rupture was studied by SEM and TEM. The results show that the alloy has excellent creep properties. Two different types of creep behavior can be shown in the creep curves. The primary creep is characterized by the high amplitude at test conditions of (760 °C, 600 MPa) and (850 °C, 550 MPa) and the primary creep strain is limited at (980 °C, 250 MPa), (1100 °C, 140 MPa) and (1120 °C, 120 MPa). A little change of γ' precipitate morphology occurs at (760 °C, 600 MPa). The lateral merging of the γ' precipitate has already begun at (850 °C, 550 MPa). The γ phase is surrounded by the γ' phase at (980 °C, 250 MPa). The γ phase is no longer continuous tested at (1070 °C, 140 MPa). At (1100 °C, 120 MPa), the thickness of γ phase continues to increase. No TCP phase precipitates in the specimens at (760 °C, 600 MPa), (850 °C, 550 MPa) and (980 °C, 250 MPa). Needle shaped TCP phase precipitates in the specimens tested at (1070 °C, 140 MPa) and (1100 °C, 120 MPa). The dislocation shear mechanism including stacking fault formation is operative at lower temperature and high stress. The dislocation by-passing mechanism occurs to form networks at γ/γ' interface under the condition of high temperature and lower stress.

Key words: single crystal superalloy; creep properties; microstructure evolution; γ' phase; TCP phase

1 Introduction

Nickel based superalloy single crystals have superior mechanical properties at elevated temperatures, which makes them the most suitable materials for the manufacture of turbine blades in aero engines. The temperature capability of the turbine blade has increased significantly for the past several decades. Some of the advances have been achieved through improving the content of refractory alloying elements [1−4]. For example, the mass fraction of refractory elements in the single crystal superalloys from the first generation to the third generation, such as CMSX-2, CMSX-4 and CMSX-10, is 14.6%, 15.4% and 20.7%, respectively [5]. The Re content in the third generation single crystal superalloys CMSX-10 [1] and RenéN6 [2] is 5.4% and 6%, respectively, which is higher than 3% in the second generation single crystal superalloys CMSX-4 and RenéN5 [5], so the temperature capability of the CMSX-10 and RenéN6 alloys has been improved by about 30 °C. However, the superalloys with high fraction refractory elements are susceptible to the precipitation of deleterious topologically close packed (TCP) phases [6,7], and the creep properties decrease as a result of the TCP formation [8,9]. The temperature and stress will influence the precipitation of TCP. Moreover, the turbine blades bear various work conditions from start to stable course and undergo the processes from medial temperature to high temperature. The single crystal superalloys with various compositions display different creep behavior [10]. Although a large amount of investigations have demonstrated the creep behavior of nickel based single crystal superalloys only at intermediate temperatures or at high temperature [10−13], few references report that the creep feature and deformation mechanisms of the alloys from medial temperature to high temperature. In this study, the creep properties of the single crystal superalloy with [001] orientation were investigated at different conditions. The microstructure evolution of γ' phase, TCP phase precipitation and dislocation characteristic after creep

Corresponding author: Zhen-xue SHI; Tel: +86-10-62498312; E-mail: shizhenxue@126.com
DOI: 10.1016/S1003-6326(14)63380-X

rupture were studied by SEM and TEM. The purpose of the investigation is to promote the development of new generation single crystal superalloy with high creep properties.

2 Experimental

Pure raw materials were used in this experimental study. A Ni−Cr−Co−Mo−W−Ta−Nb−Re−Al system single crystal with [001] orientation was cast by means of crystal selection method in the directionally solidified furnace with the temperature gradient of 80 °C/cm. The nominal chemical compositions dimension of the alloy are listed in Table 1. The crystal orientations of the specimens were determined with Laue X-ray back reflection method, and the crystal orientation deviations of the specimens were maintained within 10° from the [001] orientation. The single crystal specimens received standard heat treatment comprising of solution treatment (1340 °C, 5 h, AC) and two-step aging treatment (1120 °C, 4 h, AC) + (870 °C, 24 h, AC). The standard cylindrical specimens for creep tests were machined after heat treatment, and the creep tests were conducted at (760 °C, 600 MPa), (850 °C, 550 MPa), (980 °C, 250 MPa), (1100 °C, 140 MPa) and (1120 °C, 120 MPa) in air using DST-5 testing machine with furnace attachment. The samples were etched with solution of 5 g $CuSO_4$ + 25 mL HCl + 20 mL H_2O + 5 mL H_2SO_4 which dissolved the γ' phase. Microstructures of the creep ruptured samples were examined by S4800 scanning electron microscope (SEM). Foils for transmission electron microscopy (TEM) analysis were obtained by cutting 0.2 mm-thick discs perpendicular to the tensile axis of the specimens using electric discharge machine. Thin foils were prepared by twin-jet thinning electrolytically in the solution of 10% perchloric acid and 90% ethanol (volume fraction) at −10 °C using liquid nitrogen.

Table 1 Nominal chemical compositions of experimental alloy (mass fraction, %)

Cr	Co	Mo	W	Ta
2−4	7−10	2−5	6−9	7−10
Re	Nb	Al	Hf	Ni
3−5	0.5−1.5	5−6	0.1−0.5	Bal.

3 Results and discussion

3.1 Microstructure after heat treatment

Figure 1 shows the microstructure of the single crystal superalloy after standard heat treatment. It can be seen that the primary γ' and γ/γ' eutectic dissolve completely after the high temperature solution treatment. The cubical γ' phase is regularly arranged along [100] direction. The average length of the γ' precipitates edge is about 0.45 μm, the width of the γ matrix channel is about 0.05 μm, and the volume fraction of the γ' phase in the alloy is more than 60%.

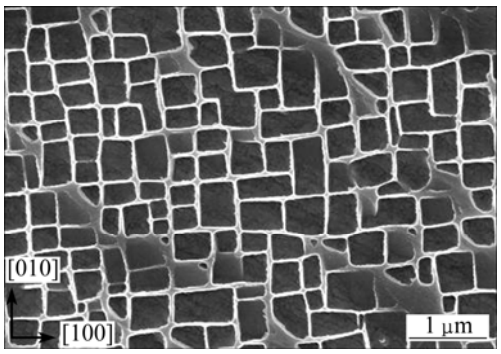

Fig. 1 Microstructure of single crystal superalloy after standard heat treatment

3.2 Creep behavior

The creep curves of the nickel-based single crystal superalloy at different test conditions are shown in Fig. 2 and the corresponding creep properties are listed in Table 2. It can be seen that the alloy has long creep life at different test conditions, which indicates that the alloy has excellent creep properties. However, two different types of creep behavior can be shown by the creep curves. The first one is characterized by the high amplitude of primary creep and another is characterized by the limited primary creep strain. At (760 °C, 600 MPa) and (850 °C, 550 MPa), the primary creep strain which is about 4% and 3% accounts for 20% and 16% of total strain, respectively. The primary creep stage amplitude is dramatically smaller at (980 °C, 250 MPa), (1100 °C, 140 MPa) and (1120 °C, 120 MPa), less than 0.3%. The secondary creep stage is quite long and the main part of the creep life corresponds to the long secondary creep stage.

3.3 Microstructure of ruptured specimens under SEM

The microstructure on the longitudinal section in the ruptured specimens of the alloy at different conditions was observed by SEM. Figure 3 shows the microstructure apart from fracture surface 1 cm of the ruptured specimens. It can be seen from the observation that a little change of γ' precipitate morphology occurs at the condition of (760 °C, 600 MPa) (Fig. 3(a)). The vertical γ matrix becomes thinner and horizontal γ matrix becomes thicker slightly. No appreciable thickening of γ' precipitates seems to have taken place. The lateral merging of the γ' precipitates has already begun along the

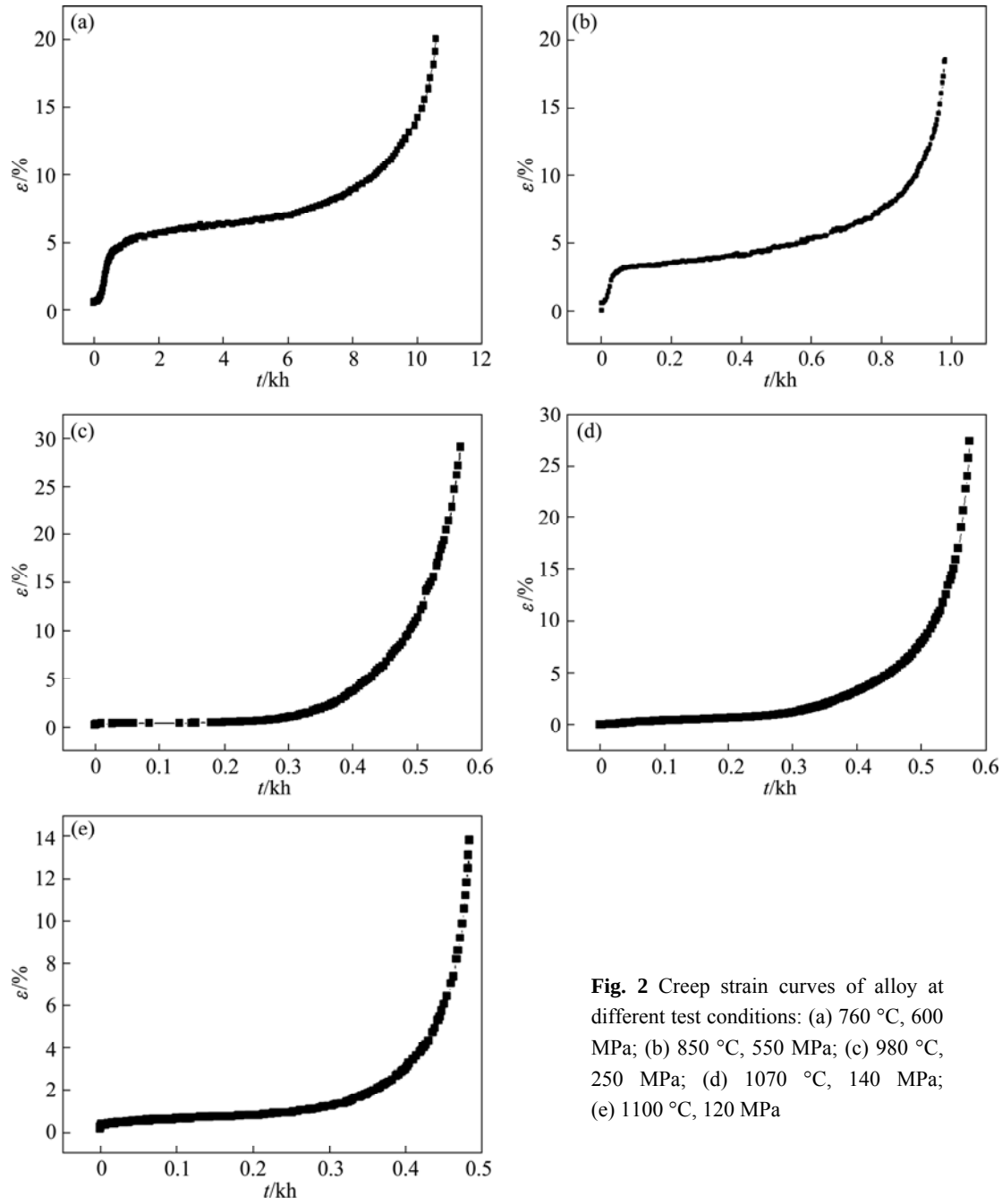

Fig. 2 Creep strain curves of alloy at different test conditions: (a) 760 °C, 600 MPa; (b) 850 °C, 550 MPa; (c) 980 °C, 250 MPa; (d) 1070 °C, 140 MPa; (e) 1100 °C, 120 MPa

Table 2 Creep properties of single crystal superalloy at different conditions

Condition	Total time to 1%/h	Total time to 2%/h	Rupture life/h	Rupture strain/%
760 °C, 600 MPa	218	317	10585.6	20.0
850 °C, 550 MPa	18	26	983.1	18.6
980 °C, 250 MPa	293	354	567.8	29.1
1070 °C, 140 MPa	282	352	576.3	27.3
1100 °C, 120 MPa	265	367	487.3	13.7

direction of the applied stress at the condition of (850 °C, 550 MPa) (Fig. 3(b)). The lateral extension of γ'precipitates is well under way. Its thickness along the direction of the applied stress increases slightly, but the striking point is the drastic thickening of the γ phase. The γ phase is surrounded by the γ' phase and forming wavy and branching platelets at condition of (980 °C, 250 MPa) (Fig. 3(c)). The feature is that the γ phase is no longer continuous at condition of (1070 °C, 140 MPa) (Fig. 3(d)). It forms islands and is thus entirely surrounded by the γ' phase. At condition of (1100 °C, 120 MPa), the thickness of γ phase continues to increase and

is generally thicker than a micron (Fig. 3(e)).

The cubic γ' phase gradually changes into raft structure because of the directional diffusion of the elements. In the process, the diffusion and redistribution of the alloying elements in the γ' and γ phases have occurred [13]. With the action of the applied stress and the misfit stress at high temperature, the forming elements Al, Ta, Nb and Hf of γ' phase diffuse to the vertical channels to promote the γ' phase growth perpendicular to [001] direction. At the same time, the forming elements Cr, Co, W, Mo and Re of γ phase diffuse to the horizontal channels in the reverse orientation to increase the width of the γ matrix. Under the condition of temperature and stress, the γ' rafted structure is gradually formed. The higher the temperature is and the faster the atoms diffuse, the faster γ' phase grows and rafts. So with the increase of temperature, the thickness of γ' rafts turns bigger.

The phase stability is the key issue for the single crystal superalloys at elevated temperatures [14]. Figure 4 shows the microstructure with TCP phase near fracture surface of the ruptured specimens. No TCP

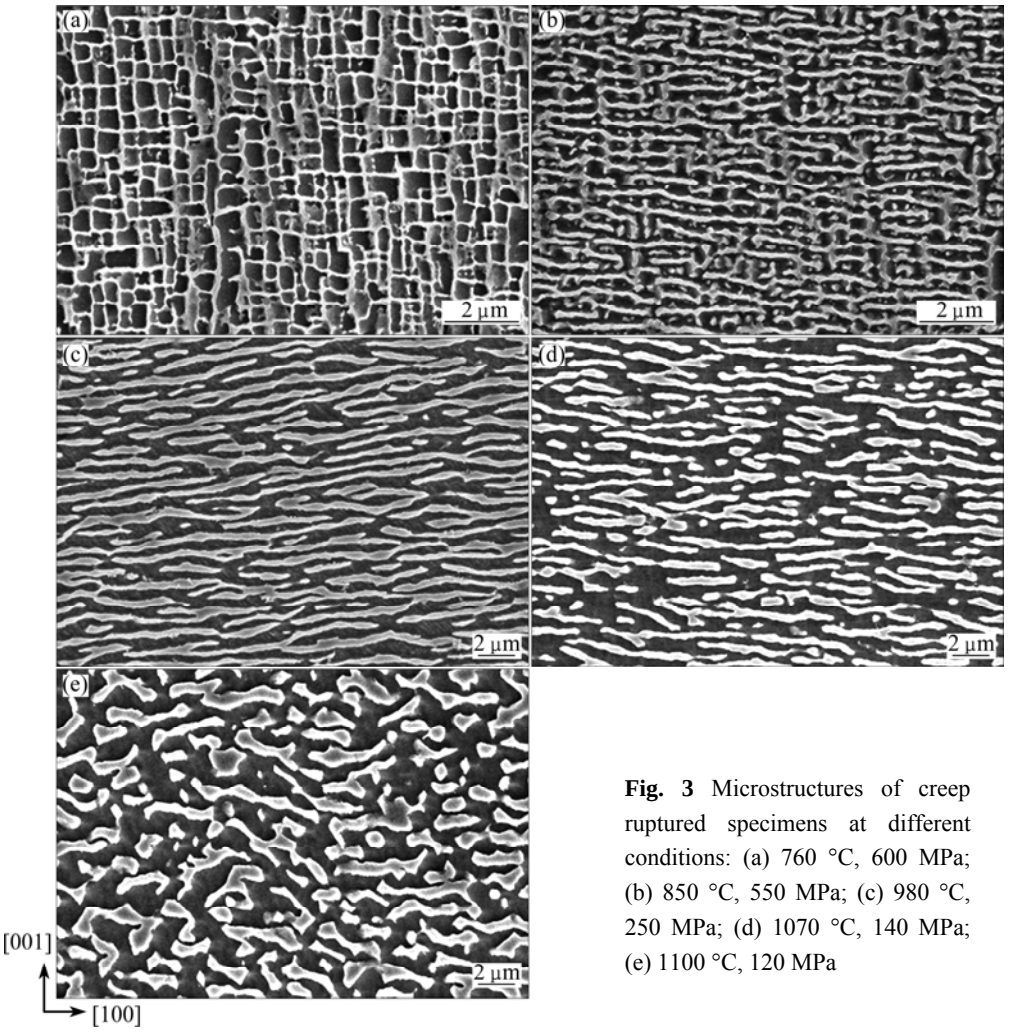

Fig. 3 Microstructures of creep ruptured specimens at different conditions: (a) 760 °C, 600 MPa; (b) 850 °C, 550 MPa; (c) 980 °C, 250 MPa; (d) 1070 °C, 140 MPa; (e) 1100 °C, 120 MPa

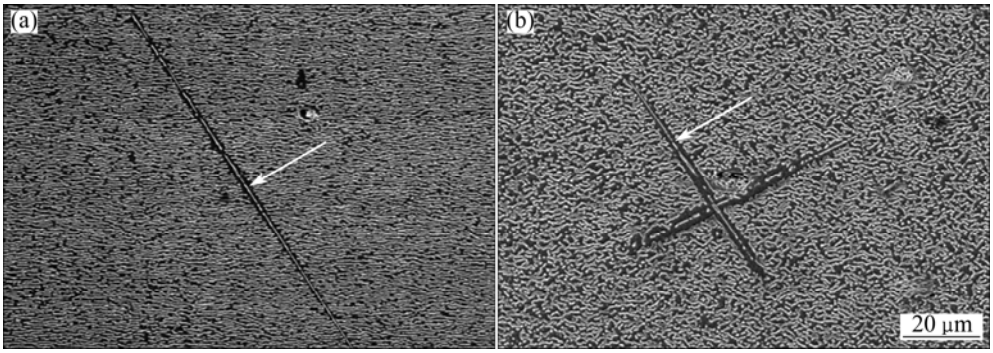

Fig. 4 TCP precipitates in creep ruptured specimens at different conditions: (a) 1070 °C, 140 MPa; (b) 1100 °C, 120 MPa

phases is observed in the ruptured specimens tested at conditions of (760 °C, 600 MPa), (850 °C, 550 MPa), (980 °C, 250 MPa). The specimens tested at (1070 °C, 140 MPa) and (1100 °C, 120 MPa) exhibit the presence of TCP phases, as shown in Fig. 4. This is caused by micro-segregation which still exists even after homogenization due to the low diffusivity of refractory elements with high melting point, such as W and Re. In addition, it is found that the TCP phase precipitates and grows along fixed direction. The chemical compositions of the TCP phase in the stress ruptured specimens tested at (1070 °C, 140 MPa) and (1100 °C, 120 MPa) are listed in Table 3, respectively. It is shown that Re and W are enriched in the TCP phase. The formation of the TCP phase in Ni-base single crystal superalloys has generally been attributed to the super-saturation of the refractory elements (Re, W) within the disordered γ phase [15]. The crystal structure of the TCP phase is extremely complex and the size of the unit cell is much larger than the lattice of the γ and γ' phases. So a large nucleation barrier serves to prevent the formation of the TCP phase in the microstructures [16]. When the TCP phase forms in the alloys, it nucleates preferentially on close-packed planes to form a semi-coherent interface, and exhibits distinctive orientation relationships with the parent crystal [17].

Table 3 Chemical composition of TCP phase in ruptured specimens (mass fraction, %)

Condition	Al	Cr	Co	Mo	Re	Ta	W	Ni
1070 °C, 140 MPa	4.18	2.12	6.84	3.18	19.29	6.11	9.51	Bal.
1100 °C, 120 MPa	5.03	2.84	7.69	3.20	20.19	5.65	12.38	Bal.

3.4 Microstructure of ruptured specimens under TEM

The creep ruptured specimens were observed by TEM. Figure 5(a) shows TEM image of creep specimen deformed at (760 °C, 600 MPa). It can be seen that a large amount of stacking faults form within the γ' phase. Super lattice intrinsic stacking faults (SISFs) are the major features of the deformation microstructure of single crystal superalloys at this condition. The high density of stacking faults indicates that cutting of γ' phase plays an important role in creep deformation under this test condition. These stacking faults lie in {111} planes and result from the shearing of the γ' precipitates by $a/3[112]$ dislocations [18]. A large amount of work has been done to study the mechanisms of stacking fault form process. A commonly observed reaction might be given by [18]

$$a/2[011]+a/2[101]\longrightarrow a/6[112]+\text{SISF}+a/3[112] \quad (1)$$

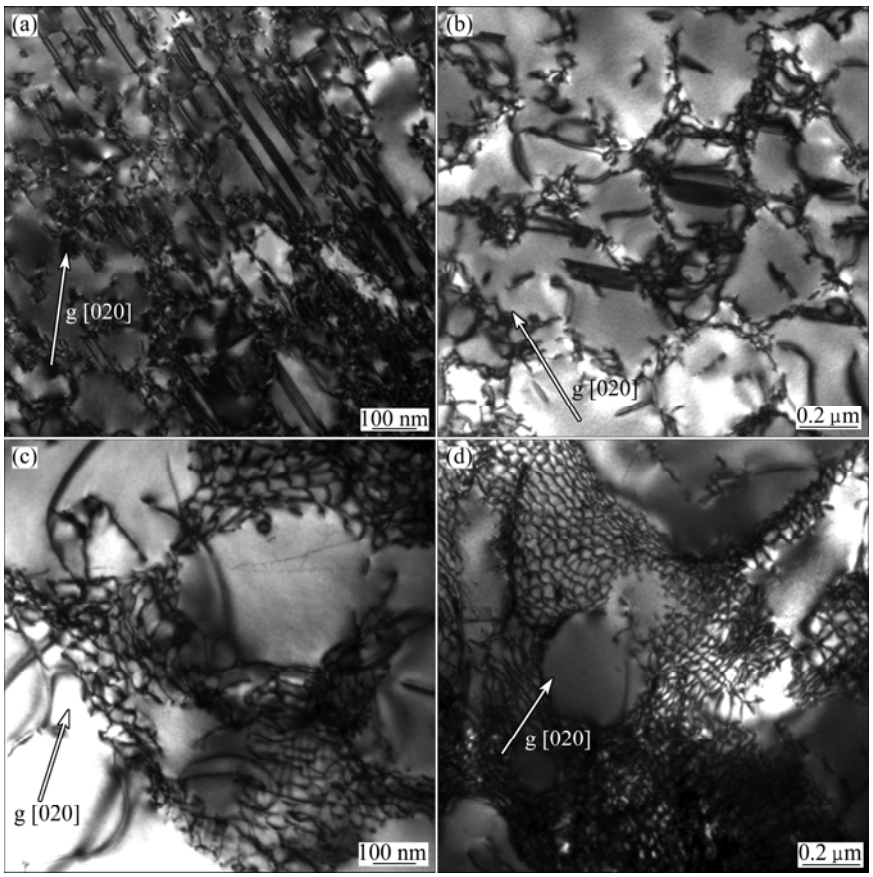

Fig. 5 TEM images of creep ruptured specimens at different condition: (a) 760 °C, 600 MPa; (b) 850 °C, 550 MPa; (c) 980 °C, 250 MPa; (d) 1100 °C, 120 MPa

Figure 5(b) shows the TEM image of creep specimen deformed at (850 °C, 550 MPa). It can be seen that the stacking fault density is low and shearing of the γ' precipitates does not seem to be the creep deformation controlling mechanism at this test condition. Some dislocations are piled up in the γ matrix channels and the interfacial regions of γ/γ' phases. In some places they have formed the dislocations tangles. And a few dislocations cut into the γ' phase.

Figures 5(c) and (d) show the morphologies of γ/γ' interfacial dislocation of creep ruptured specimens at (980 °C, 250 MPa) and (1100 °C, 120 MPa), respectively. It can be seen that the hexagonal array of dislocation networks are obviously formed at interfaces for different specimens. At high temperature, dislocations and interfaces provide increased diffusion promoting by-passing of the γ' phase by climbing [19]. The deformation feature of the alloy is the movement of 1/2[110] dislocations on the octahedral slip systems in the matrix channels [20]. The dislocation networks in matrix result from the reaction of two sets dislocations with different Burgers vectors during creep. These dislocations exist in the different slip plane. Once these dislocations move to the same slip plane to come across each other, the three-dimensional networks may be formed by the reaction of dislocation, as shown in Fig. 6.

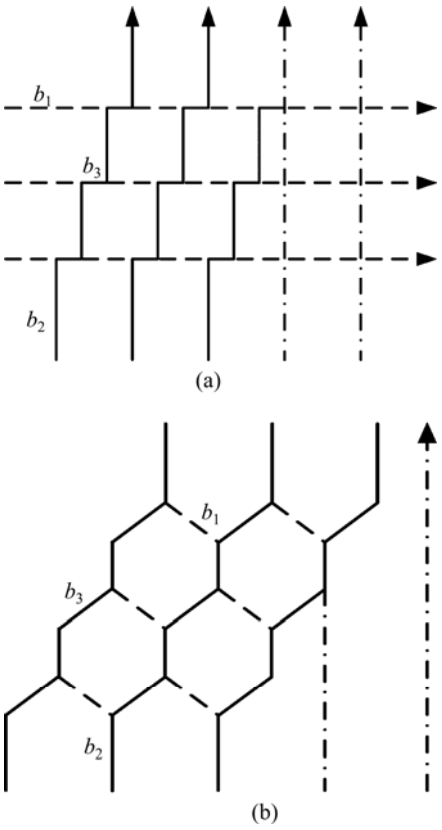

Fig. 6 Schematic diagram of dislocation networks formed by reaction [15]: (a) Before formation of dislocation networks; (b) Dislocation networks

The dislocations b_1 and b_2 meet and react to form dislocation b_3. Because of the line tension, the three sets of dislocations exist at an angle of 120° at the equilibrium state of the networks. The dislocation reaction occurs at the network as follows [20]:

$$a/2[1\bar{1}0]+a/2[011]\longrightarrow a/2[101] \quad (2)$$

The dense γ/γ' interfacial dislocation networks can be a sessile dislocation substructure which provides strengthening by affecting the strength of the γ/γ' interface and by interacting with mobile dislocations. They can effectively prevent the dislocation from cutting into γ' phase in the creep process [21]. In the later creep process, the deformation feature of the alloy is the shearing of γ' rafts by dislocations from the interfaces where networks are damaged. It can be seen in Figs. 5(c) and (d) that some dislocations cut into the γ' phase.

The TCP phase precipitating in creep ruptured specimen at (1100 °C, 120 MPa) was investigated by TEM. The selected area electron diffraction (SAED) patterns were used to determine the lattice cells (for the identification) of the TCP phases, as shown in Fig. 7. The crystal structure of TCP phase in the alloy is determined to be the σ phase, which precipitates and grows along fixed direction, $[112]_\sigma // [001]_\gamma$ and $(1\bar{1}0)_\sigma // (2\bar{2}0)_\gamma$.

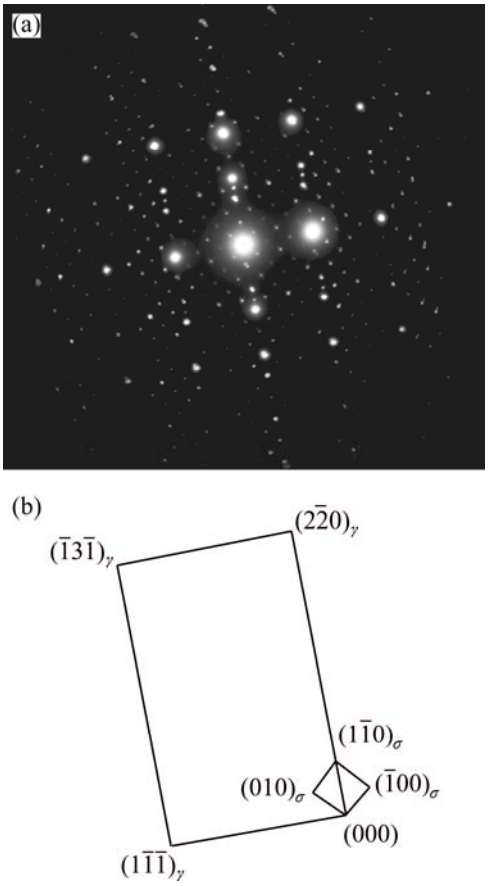

Fig. 7 SAED pattern of TCP phase in creep ruptured specimen at (1100 °C, 120 MPa)

4 Conclusions

1) Two different types of creep behavior can be shown in the creep curves. The primary creep was characterized by high amplitude at (760 °C, 600 MPa) and (850 °C, 550 MPa), and the primary creep strain is limited at test conditions of (980 °C, 250 MPa), (1100 °C, 140 MPa) and (1120 °C, 120 MPa).

2) A little change of γ' precipitate morphology occurs at (760 °C, 600 MPa). The lateral merging of the γ' precipitate has already begun at (850 °C, 550 MPa). The γ phase is surrounded by the γ' phase at (980 °C, 250 MPa). The γ phase is no longer continuous at (1070 °C, 140 MPa). At (1100 °C, 120 MPa), the thickness of γ phase continues to increase. With the rise of temperature, the thickness of γ' rafts turns bigger.

3) No TCP phase precipitates in the specimens tested at (760 °C, 600 MPa), (850 °C, 550 MPa) and (980 °C, 250 MPa). Needle shaped TCP phase precipitates in the specimens tested at (1070 °C, 140 MPa) and (1100 °C, 120 MPa). TCP phase is identified as σ phase which is mainly composed of Re and W.

4) The dislocation shear mechanism including stacking fault formation is operative at lower temperature and high stress. The dislocation by-passing mechanism begins to form networks at γ/γ' interface under the condition of high temperature and lower stress.

References

[1] WALSTON W S, O'HARA K, ROSS E W, POLLOCK T M, MURPHY W H. RenéN6: Third generation single crystal superalloy [C]//KISSINGER R D, DEYE D J, ANTON D L, CETEL A D, NATHAL M V, POLLOCK, T M, WOODFORD D A. Superalloys. Warrendale: TMS, 1996: 27−34.

[2] ERICKSON G L. The development and application of CMSX-10 [C]//KISSINGER R D, DEYE D J, ANTON D L, CETEL A D, NATHAL M V, POLLOCK, T M, WOODFORD D A. Superalloys. Warrendale: TMS, 1996: 35−44.

[3] ARGENCE D, VERNAULT C, DESVALLEES Y, FOURNIER D. MC-NG: Generation single crystal superalloy for future aeronautical turbine blades and vanes [C]//POLLOCK T M. Superalloys. Warrendale: TMS, 2000: 829−837.

[4] WALSTON S, CETEL A, MACKAY R, O'HARA K, DUHL D, DRESHFIELD R. Joint development of a fourth generation single crystal superalloy [C]//GREEN K A, POLLOK T M, HARADA H, HOWSON T W, REED R C, SCHIRRA J J, WALSTON S. Superalloys. Pennsylvania: TMS, 2004: 15−24.

[5] CARON P, KHAN T. Evolution of Ni-based superalloys for single crystal gas turbine blade applications [J]. Aerospace Science Technology, 1999, 3: 513−523.

[6] ACHARYA M V, FUCHS G E. The effect of long term thermal exposures on the microstructure and properties of CMSX-10 single crystal superalloys [J]. Materials Science and Engineering A, 2004, 381: 143−153.

[7] CHATTERJEE D, HAZARI N, DAS N, MITRA R. Microstructure and creep behavior of DMS4-type nickel based superalloy single crystals with orientations near [001] and [011] [J]. Materials Science and Engineering A, 2010, 528: 604−613.

[8] YEH A C, TIN S. Effect of Ru on the high temperature phase stability of Ni-base single crystal superalloys [J]. Metallurgical and Materials Transactions A, 2006, 37: 2621−2631.

[9] HOBBS R A, ZHANG L, RAE C M F, TIN S. The effect of ruthenium on the intermediate to high temperature creep response of high refractory content single crystal suepralloy [J]. Materials Science and Engineering A, 2008, 489: 65−76.

[10] TIAN S G, ZHENG Z, LIANG F S, CHAO Z, CHEN L. Creep behavior of a 4.5%-Re single crystal nickel-based superalloy at intermediate temperatures [J]. Materials Science and Engineering A, 2012, 543: 104−109.

[11] YU X F, DU H Q, TIAN S G, NING Y, WANG T J, CUI S S. Creep deformation mechanism in Re free second generation nickelbase single crystal superalloy during medium temperature and high stress [J]. The Chinese Journal of Nonferrous Metals, 2012, 21(7): 1921−1928. (in Chinese)

[12] WANG K G, LI J R. Study on creep properties of single crystal superalloy DD6 at 980 °C [J]. Journal of Material Engineering, 2004, 8: 7−11. (in Chinese)

[13] TIAN S G, ZHANG J H, ZHOU H H, YANG H C, XU Y B, HU Z Q. Aspects of primary creep of a single crystal nickel-base superalloy [J]. Materials Science and Engineering A, 1999, 262: 271−278.

[14] SHI Z X, LI J R, LIU S Z, WANG X G, YUE X D. Effect of Ru on stress rupture properties of nickel-based single crystal superalloy at high temperature [J]. Transactions of Nonferrous Metals Society of China, 2012, 22: 2106−2111.

[15] CARROLL L J, FENG Q, MANSFIELD J F, POLLOCK T M. Elemental partitioning in Ru-containing Nickel-base single crystal superalloys [J]. Materials Science and Engineering A, 2009: 457: 292−299.

[16] NEUMEIER S, PYCZAK F, GÖKEN M. The influence of ruthenium and rhenium on the local properties of the γ- and γ'-phase in Nickel-base superalloys and their consequences for alloy behavior [C]//REED R C, GREEN K A, CARON P, GABB P, FAHRMANN G, HURON E S, WOODARD S A. Superalloys. Pennsylvania: TMS, 2008: 109−110.

[17] RAE C M F, KARUNARATNE M S A, SMALL C J, BROOMFIELD R W, JONES C N, REED R C. Topologically close packed phases in an experimental Rhenium-containing single crystal superalloy [C]//Pollock T M, KISSINGER R D, BOWMAN R R, GREEN K A, MCLEAN M, OLSON S, SCHIRRA J J. Superalloys. Warrendale: TMS, 2000: 767−777.

[18] RAE C M F, REED R C. Primary creep in single crystal superalloys: Origins, mechanisms and effects [J]. Acta Materialia, 2007, 55: 1067−1081.

[19] TIAN S G, ZHANG J H, ZHOU H H, YANG H C, XU Y B, HU Z Q. Formation and role of dislocation networks during high temperature creep of a single crystal nickel–base superalloy [J]. Materials Science and Engineering A, 2000, 279: 160−165.

[20] YU J J, SUN X F, JIN T, ZHAO N R, GUAN H R, HU Z Q. High temperature creep and low cycle fatigue of a nickel-base superalloy [J]. Materials Science and Engineering A, 2010, 527: 2379−2389.

[21] ZHANG J X, MURAKUMO T, KOIZUMI Y, KOBAYASHI T, HARADA H, MASAKI S. Interfacial dislocation networks strengthening a fourth-generation single-crystal TMS-138 superalloy [J]. Metallurgical and Materials Transactions A, 2002, 33: 3741−3746.

镍基单晶高温合金在不同条件下的蠕变性能和组织演化

史振学，李嘉荣，刘世忠，王效光

北京航空材料研究院 先进高温结构材料重点实验室，北京 100095

摘 要：研究[001]取向的镍基单晶高温合金在不同测试条件下的蠕变性能，采用扫描电镜和透射电镜研究合金蠕变断裂后的 γ′相、TCP 相和位错组织演化特征。结果表明：合金具有良好的蠕变性能，蠕变曲线显示出两种不同的蠕变变形特征。在(760 °C, 600 MPa)、(850 °C, 550 MPa)条件下，蠕变第一阶段较长；在(980 °C, 250 MPa)、(1070 °C, 140 MPa)和(1100 °C, 120 MPa)条件下，蠕变第一阶段很短。蠕变断裂后，在(760 °C, 600 MPa)条件下 γ′相形态变化不大；在(850 °C, 550 MPa)条件下 γ′相已经合并长大；在(980 °C, 250 MPa)条件下基体 γ 被 γ′相包围；在(1070 °C, 140 MPa)条件下基体 γ 不再连续；在(1100 °C, 120 MPa)条件下基体 γ 厚度进一步增加。在(760 °C, 600 MPa)、(850 °C, 550 MPa)和(980 °C, 250 MPa)条件下合金无 TCP 相析出，而在(1070 °C, 140 MPa)和(1100 °C, 120 MPa)条件下有针状 TCP 相析出。在低温高应力下，变形特征为位错包括层错的剪切机制；在高温低应力下为位错绕过机制，并在 γ/γ′相界面形成位错网。

关键词：单晶高温合金；蠕变性能；组织演化；γ′相；TCP 相

(Edited by Chao WANG)